How to cite: *Angew. Chem. Int. Ed.* **2025**, *64*, e202416781
doi.org/10.1002/anie.202416781

Strained Molecules

Stereoselective Radical Acylfluoroalkylation of Bicyclobutanes via N-Heterocyclic Carbene Catalysis

Chuyu Xiao[+], Jing-Ran Shan[+], Wen-Deng Liu, Xingyuan Gao, Jingwei Dai, Zuwei Wang, Wentao Wang, K. N. Houk, and Jiannan Zhao**

Abstract: Cyclobutanes are prominent structural components in natural products and drug molecules. With the advent of strain-release-driven synthesis, ring-opening reactions of bicyclo[1.1.0]butanes (BCBs) provide an attractive pathway to construct these three-dimensional structures. However, the stereoselective difunctionalization of the central C–C σ-bonds remains challenging. Reported herein is a covalent-based organocatalytic strategy that exploits radical NHC catalysis to achieve diastereoselective acylfluoroalkylation of BCBs under mild conditions. The Breslow enolate acts as a single electron donor and provides an NHC-bound ketyl radical with appropriate steric hindrance, which effectively distinguishes between the two faces of transient cyclobutyl radicals. This operationally simple method tolerates various fluoroalkyl reagents and common functional groups, providing a straightforward access to polysubstituted cyclobutanes (75 examples, up to >19:1 d.r.). The combined experimental and theoretical investigations of this organocatalytic system confirm the formation of the NHC-derived radical and provide an understanding of how stereoselective radical-radical coupling occurs.

Introduction

Cyclobutanes constitute an important structural motif found in numerous biologically active natural products.[1] Their favorable physicochemical properties, along with their utility as functional group bioisosteres, render them particularly attractive in the context of drug discovery.[2] Consequently, the development of new strategies for the efficient and rapid synthesis of these three-dimensional structures has garnered considerable attention from the synthetic chemistry community.[3,4] The most straightforward strategies for synthesizing cyclobutanes involve [2+2] cycloadditions of alkenes, facilitated by Lewis acid catalysis or photocatalysis.[4] Furthermore, with the emergence of strain-release-driven synthesis,[5] bicyclo[1.1.0]butanes (BCBs) have gained prominence as versatile precursors, offering a divergent pathway for the construction of these carbocycles.[6–8]

The reactivity of the BCB scaffold involves mainly its central C–C bond (Figure 1A). Regioselective ring-opening of this bond has been achieved by both nucleophiles[6a–f] and electrophiles.[6h] Moreover, recent advancements in photocatalysis have enabled radical-involved difunctionalization of these strained σ-bonds, presenting an attractive approach to access polysubstituted cyclobutanes.[7] However, controlling diastereoselectivity (*syn* vs *anti*) in this process remains a considerable challenge.[7a,b] This is largely due to the limited interaction between the photocatalyst and the radical-based intermediates, which undergo the reaction with minimal activation barriers. In a notable report, Aggarwal demonstrated that the central C–C bond in boronate-substituted BCBs was readily cleaved by electrophilic radicals (Figure 1B, path i).[7c,d] The radical addition led to the formation of an α-boryl radical intermediate, inducing a stereospecific 1,2-migration of the boron substituent to the α-carbon. More recently, Glorius and coworkers have explored the reaction of BCBs with sulfur-containing bifunctional reagents under photoredox conditions (Figure 1B, path ii).[7e] The cleavage of C–S σ-bonds in the cyclic radical cationic intermediates resulted in *syn*-selective thio-carbofunctionalization of the strained C−C bond. While these approaches have achieved impressive diastereoselectivities with carefully designed substrates, the development of methods that utilize stereodifferentiating catalysts is less developed.

N-Heterocyclic carbene (NHC) radical organocatalysis has recently emerged as a powerful platform for the invention of versatile transformations.[9–13] The Breslow enolate **A**, generated upon nucleophilic addition of an NHC to an aldehyde, is recognized as a potent reductant ($E_{1/2}$[**B**/**A**] = −1.2~−1.7 V vs SCE),[10] capable of initiating single-electron transfer (SET) with appropriate redox partners (Figure 1C).[11] A primary reaction pathway involves the addition of the generated radicals to styrene, leading to the

[*] C. Xiao,[+] W.-D. Liu, X. Gao, J. Dai, Prof. Dr. J. Zhao
School of Chemistry
Dalian University of Technology
Dalian 116024 (China)
E-mail: jnzhao@dlut.edu.cn

J.-R. Shan,[+] Z. Wang, Prof. Dr. K. N. Houk
Department of Chemistry and Biochemistry
University of California, Los Angeles
Los Angeles, CA 90095 (USA)
E-mail: houk@chem.ucla.edu

Prof. Dr. W. Wang
Dalian Institute of Chemical Physics
Chinese Academy of Sciences
Dalian 116023 (China)

[+] These authors contributed equally to this work

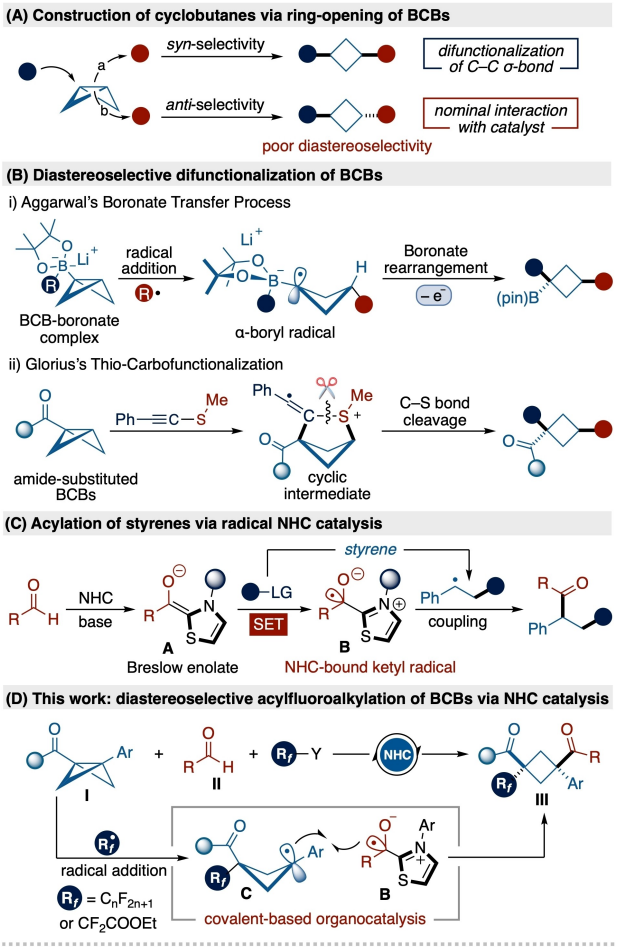

Figure 1. Stereoselective construction of cyclobutanes via acylfluoroalkylation of BCBs.

formation of a more stable benzyl radical. This radical subsequently undergoes cross-coupling with the NHC-derived ketyl radical **B**, achieving the difunctionalization of the C=C bond. Furthermore, since the ketyl radical was covalently bound to the organocatalyst, this strategy allowed us to develop stereoselective radical-radical coupling reactions.[11g,12i,j] In contrast to the extensively studied NHC-catalyzed radical acylation reactions of π-systems (e.g. alkenes, alkynes, allenes), we explored the covalent-based organocatalytic strategy for the stereoselective acylation of the BCB group (Figure 1D).

Based on the above hypothesis, we speculated that electrophilic fluoroalkyl radicals ($R_f^{\bullet}$), generated via NHC-catalyzed SET reduction,[13] could trigger radical ring-opening reactions of BCBs, leading to the formation of benzyl radicals **C**. We envisioned that the ensuing NHC-bound ketyl radical **B** could differentiate between competing stereomeric transition states of the transient cyclobutyl radical **C**, thereby enabling diastereoselective acylfluoroalkylation of BCBs. This organocatalytic protocol provides access to polysubstituted cyclobutanes, which can be further transformed into oxa-bridged bicyclic structures. Integrated experimental, computational, and spectroscopic studies substantiated the formation of the NHC-derived radical and elucidated the origin of stereocontrol.

Results and Discussion

Reaction Development

Figure 2 depicts our proposed catalytic cycle, which is initiated by the formation of Breslow enolate **A** through the nucleophilic addition of a thiazolium-derived NHC to aldehyde **1** in the presence of a base. This step is followed by the SET reduction of the fluoroalkyl source **3** (R_f-Y), converting enolate **A** into a ketyl radical **B**. The subsequent addition of the fluoroalkyl radical to the central C–C bond of BCB **2** delivers the benzyl radical **C**, which would undergo diastereoselective radical cross-coupling with the NHC-bound radical **B**. Finally, the elimination of NHC from intermediate **D** affords the fluorine-containing cyclobutane **4** and completes the catalytic cycle.

The feasibility of the organocatalytic plan was evaluated by exploring the reaction of 1,3-disubstituted BCB **2a** with benzaldehyde **1a** (Table 1). The Togni **I** reagent **3a** was initially selected as the fluoroalkyl source due to its ability to participate in SET with Breslow enolates. Upon optimizing various reaction parameters, the desired carbocycle **4** was obtained in 81 % isolated yield after reaction under a nitrogen atmosphere for 18 hours (entry 1). Remarkably, in alignment with our expectations, the tetrasubstituted cyclobutane **4** was isolated as a single diastereomer with >19:1 d.r., when employing *N*-2,4,6-trimethylphenyl-substituted thiazolium salt **N1** as the catalyst. Further investigation of the catalyst revealed that the use of either *N*-neopentyl-substituted **N3** or *N*-benzyl-substituted **N4** resulted in diminished diastereoselectivies (entries 3 and 4). These outcomes suggested that steric hindrance adjacent to the NHC moiety plays a critical role in dictating stereocontrol. Additionally, alternative trifluoromethyl sources, such as the Togni **II** reagent and Umemoto's reagent, were found to significantly compromise the reaction yield (entries 5 and 6).

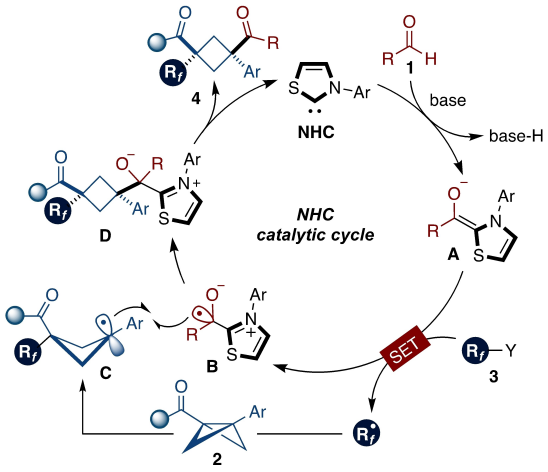

Figure 2. Prospective catalytic cycle.

Table 1: Investigation of the reaction parameters.[a]

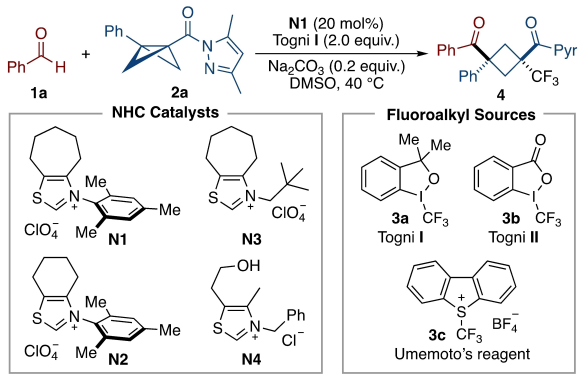

entry	variation from above conditions	yield [%][b]	d.r.[c]
1	none	81	>19:1
2	**N2** instead of **N1**	50	>19:1
3	**N3** instead of **N1**	29	6:1
4	**N4** instead of **N1**	37	4:1
5	**3b** instead of **3a**	N.R.	–
6	**3c** instead of **3a**	N.R.	–
7	Cs_2CO_3 instead of Na_2CO_3	56	>19:1
8	$NaHCO_3$ instead of Na_2CO_3	38	>19:1
9	CH_3CN instead of DMSO	Trace	–
10	DMF instead of DMSO	30	>19:1

[a] The reactions were carried out with **1a** (0.1 mmol), **2a** (0.2 mmol), **3a** (0.2 mmol), NHC catalyst (20 mol%) and Na_2CO_3 (20 mol%) in 1.0 mL of DMSO at 40 °C for 18 h. [b] Yields of isolated products. [c] Diastereomeric ratio (d.r.) values were determined by ^{1}H NMR.

Switching the base to either Cs_2CO_3 or $NaHCO_3$ yielded inferior results compared to the optimized result (entries 7 and 8). Further examination of different solvents highlighted DMSO as the superior solvent for this transformation (entries 9 and 10).

Substrate Scope

Upon establishing the optimized conditions, we proceeded to investigate the scope and limitations of the organocatalytic acylfluoroalkylation reaction. The observed excellent stereoselectivity prompted us to initially examine the reaction of bicyclobutane **2a** with a diverse array of aldehydes (Scheme 1). The NHC catalyzed radical reaction proved effective with a broad spectrum of aryl aldehydes, yielding the corresponding cyclobutane derivatives with satisfying yields and consistently high diastereoselectivities (**5**–**35**). The reaction outcomes were influenced by the positions of the substituents on the aromatic ring. Generally, benzaldehydes bearing *para*-substitutions afforded the desired products (**10**–**14**) in better yields compared to their *meta*-substituted analogues (**5**–**9**). In line with previous studies,[11] aldehydes featuring *ortho*-substituted aromatic rings were sterically challenging under current reaction conditions.[14] X-ray crystallographic analysis of compound **4** unequivocally demonstrated that the *N*-acylpyrazole and carbonyl groups are positioned *cis* to each other on the cyclobutane scaffold. Notably, our research has effectively incorporated a spectrum of functionalities, such as nitrile, ester, thioether, sulfonyl, and trifluoromethyl groups (**17**–**23**), which are frequently employed in medicinal chemistry. The reaction with *para*-B(pin)-benzaldehyde yielded product **24**, which is amenable to conventional cross-coupling chemistry. Furthermore, the stereoselective transformation proceeded smoothly with 2-naphthaldehyde (**25**) and various heteroaryl aldehydes, encompassing derivatives of pyridine (**26**–**28**), furan (**29**) and thiophene (**30**). In addition to aromatic aldehydes, the organocatalytic system also allowed the use of aliphatic aldehydes as the acyl source (**31**–**32**), albeit with lower yields. The broad functional group compatibility of the reaction prompted us to explore its practicality for late-stage functionalization of biorelevant compounds. Aldehydes derived from dicamba, gemfibrozil, and estrone also underwent the acylfluoroalkylation reaction efficiently, affording the corresponding products (**33**–**35**) with complete diastereoselectivity and yields ranging from 54% to 81%.

Upon investigating the scope of aldehydes, we turned our attention to the compatibility of this diastereoselective acylfluoroalkylation reaction with other bicyclobutanes (Scheme 2). To this end, modifications on both the aromatic ring (R^1) and the carbonyl moiety (R^2) were investigated. As summarized in Scheme 2, variations in the electronic characteristics of substituents on the aryl moiety exerted a minimal impact on the reaction efficiency (**36**–**44**). Ester-substituted bicyclobutanes readily participated in the reaction, furnishing the desired product (**45**) in good yields. Unfortunately, BCB with an alkyl substituent (R^1=Me) was not successful, presumably due to the instability of the cyclobutyl radical generated by ring-opening.[15] Next, we evaluated the influence of electron-withdrawing substituents at the bridgehead of BCB. All explored cyclic amides were found to be compatible with this organocatalytic system (**46**–**48**), affording the corresponding products in good yields. Furthermore, the successful incorporation of Weinreb amide (**49**) underscores the functional group tolerance of our method, offering a versatile platform for subsequent chemical modifications. Apart from the amide, ester functionalized BCBs were also successfully employed (**50**–**52**), although only moderate levels of diastereoselectivity were achieved. Furthermore, BCBs featuring aromatic ketones underwent the reaction smoothly, delivering the products (**53**–**55**) in good yields and diastereocontrol.

Considering the significance of fluoroalkyl-substituted organic compounds in the pharmaceutical and agrochemical industries,[16] we endeavored to expand the applicability of this organocatalytic strategy to incorporate other fluoroalkyl groups onto cyclobutanes (Scheme 3). It was gratifying to find that this method was applicable to the construction of the difluoromethyl-substituted cyclobutanes **56** using $BrCF_2COOEt$, albeit with an initially low yield. Further optimization of the reaction conditions, particularly the addition of Li_2CO_3, significantly improve the yield to 72%. When these modified conditions were extended to aldehydes with either electron-rich or electron-deficient groups at the *para*-position, the cyclic products **57**–**60** were obtained in good yields with >19:1 d.r. Notably, this strategy also

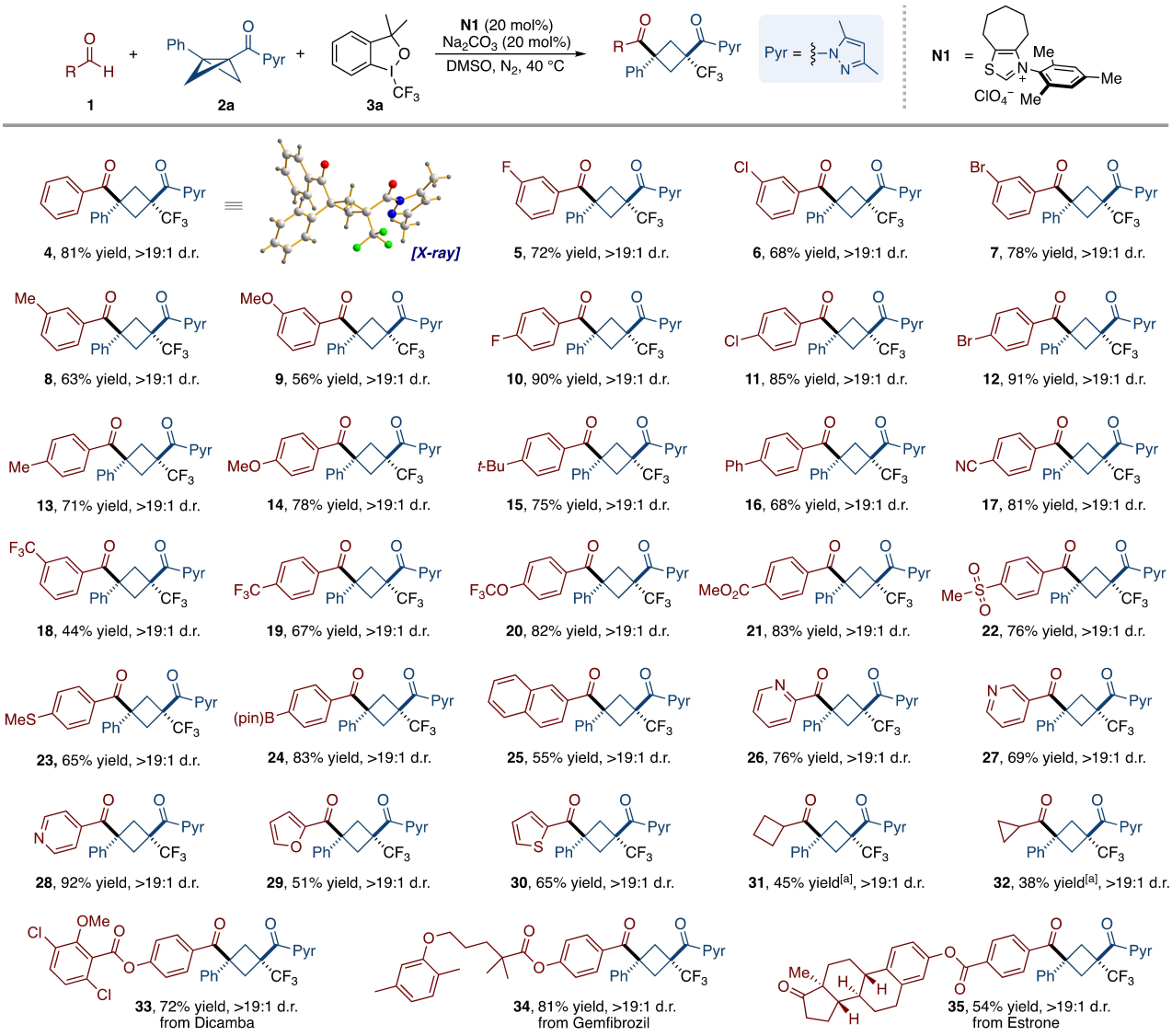

Scheme 1. Scope of aldehydes. Reactions generally performed with aldehyde **1** (0.1 mmol), bicyclobutane **2a** (0.2 mmol), Togni **I** reagent **3a** (0.2 mmol), NHC precatalyst **N1** (20 mol%) and Na_2CO_3 (20 mol%) in DMSO (1.0 mL) at 40 °C for 18 h. Isolated product yields. Diastereomeric ratio (d.r.) values were determined by ^1H NMR. [a] Reactions were carried out with aliphatic aldehyde **1** (0.15 mmol), bicyclobutane **2a** (0.1 mmol) and Na_2CO_3 (50 mol%).

proved compatible with both acyclic and cyclic aliphatic aldehydes, which efficiently coupled with BCB to produce difluoroalkyl-substituted carbocycles (**61**–**65**) with excellent diastereoselectivities. Encouraged by these promising results, we proceeded to explore the perfluoroalkylation of BCBs. As further illustrated in Scheme 3, a variety of accessible perfluoroalkyl iodides, with varying fluoroalkyl chain lengths, proved to be suitable substrates in this NHC organocatalytic system, providing the perfluorinated cyclobutanes in 33%–74% yields (**75**–**78**).

Synthetic Applications

To demonstrate the practicality of this organocatalytic reaction, we conducted a gram-scale synthesis (Scheme 4A). Bicyclobutane **2a** (5.0 mmol) reacted smoothly with benzaldehyde **1a** and Togni **I** reagent under standard conditions, affording the carbocycle **4** in 66% yield (1.41 g). Taking advantage of the *cis* configuration of the carbonyl moieties, manipulation of the cyclic products facilitated the synthesis of bicyclic scaffolds (Scheme 4B). Treatment of **4** with $NaBH_4$ afforded diol **79**, which subsequently underwent dehydration with triflic acid (TfOH) to afford 3-oxabicyclo-[3.1.1]heptane derivative **80**. Additionally, selective reduction of **50**, followed by transesterification, yielded the bridged [3.1.1] bicyclic lactone **81**, whose structure was

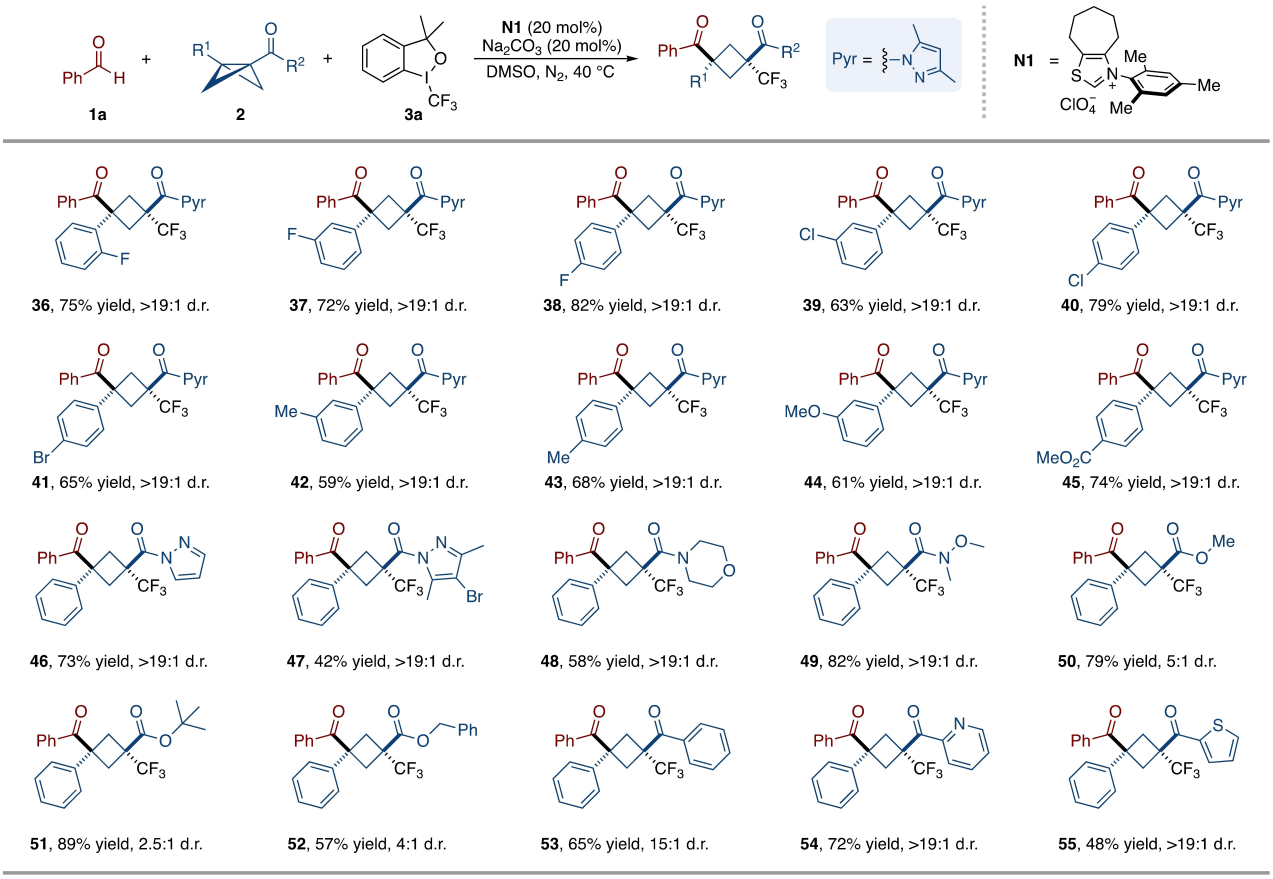

Scheme 2. Scope of bicyclobutanes. Reactions generally performed with benzaldehyde **1a** (0.1 mmol), bicyclobutane **2** (0.2 mmol), Togni **I** reagent **3a** (0.2 mmol), NHC precatalyst **N1** (20 mol%) and Na_2CO_3 (20 mol%) in DMSO (1.0 mL) at 40 °C for 18 h. Isolated product yields. Diastereomeric ratio (d.r.) values were determined by ^1H NMR.

confirmed by X-ray crystallographic analysis. Since the cyclobutyl moiety frequently acts as an aryl ring isostere,[2] the ester-containing product **45** was converted to the amide **82**, which may exhibit potential affinity for the histamine H_3 receptor.[17]

Experimental Investigations on the Reaction Pathways

To support the mechanism suggested in Figure 2, a radical-trapping experiment was performed. As illustrated in Scheme 5A, the transformation was completely inhibited by the addition of a stoichiometric amount of 2,2,6,6-tetramethyl-1-piperidinyloxy (TEMPO). The alkyl radical-TEMPO trapping adduct **84** was observed by HRMS analysis, suggesting a radical nature of the reaction pathway. To further investigate the involvement of the NHC-bound ketyl radical **B**, a mixture of the NHC precatalyst **N1** in DMSO with equimolar amounts of PhCHO, Togni **I** reagent, and Na_2CO_3 was analyzed by electron paramagnetic resonance (EPR) spectroscopy (Scheme 5B, path a).[10,18] The observation of a strong EPR signal clearly indicated the generation of a radical species. Additionally, we attempted to prepare the acyl thiazolium **E** in situ from **N1** and benzoyl chloride (Scheme 5B, path b). We proposed that the SET reduction of intermediate **E** would also produce the ketyl radical **B**. As expected, the EPR spectrum of the solution was identical to previous observations. All these results are in line with our suggested mechanism and strongly support the formation of the ketyl radcial **B**.

Computational Studies

Density functional theory (DFT) calculations were performed to investigate the proposed mechanism using **1a** and **2a** as model substrates (Scheme 6). Nucleophilic addition of NHC catalyst **N1'** to **1a** readily proceeds via **TS1** with an energy barrier of 18.5 kcal/mol, forming the zwitterionic intermediate **IN1**, which is subsequently deprotonated by Na_2CO_3. The Breslow enolate **IN2** undergoes SET with Togni **I** reagent **3a** to form ketyl radical **IN3**, while Togni **I** reagent undergoes fragmentation to **IN4** and the trifluoromethyl radical **IN5**. The SET process is exergonic by 13.2 kcal/mol. Attack of trifluoromethyl radical **IN5** on BCB **2a** via **TS2** has an energy barrier of 10.9 kcal/mol, elongating the BCB C–C bond from 1.53 Å to 1.63 Å. This strain-release step is exergonic by 55.0 kcal/mol, irreversibly resulting in the formation of stable benzyl radical **IN6** as the other coupling species. The radical-radical cross-coupling

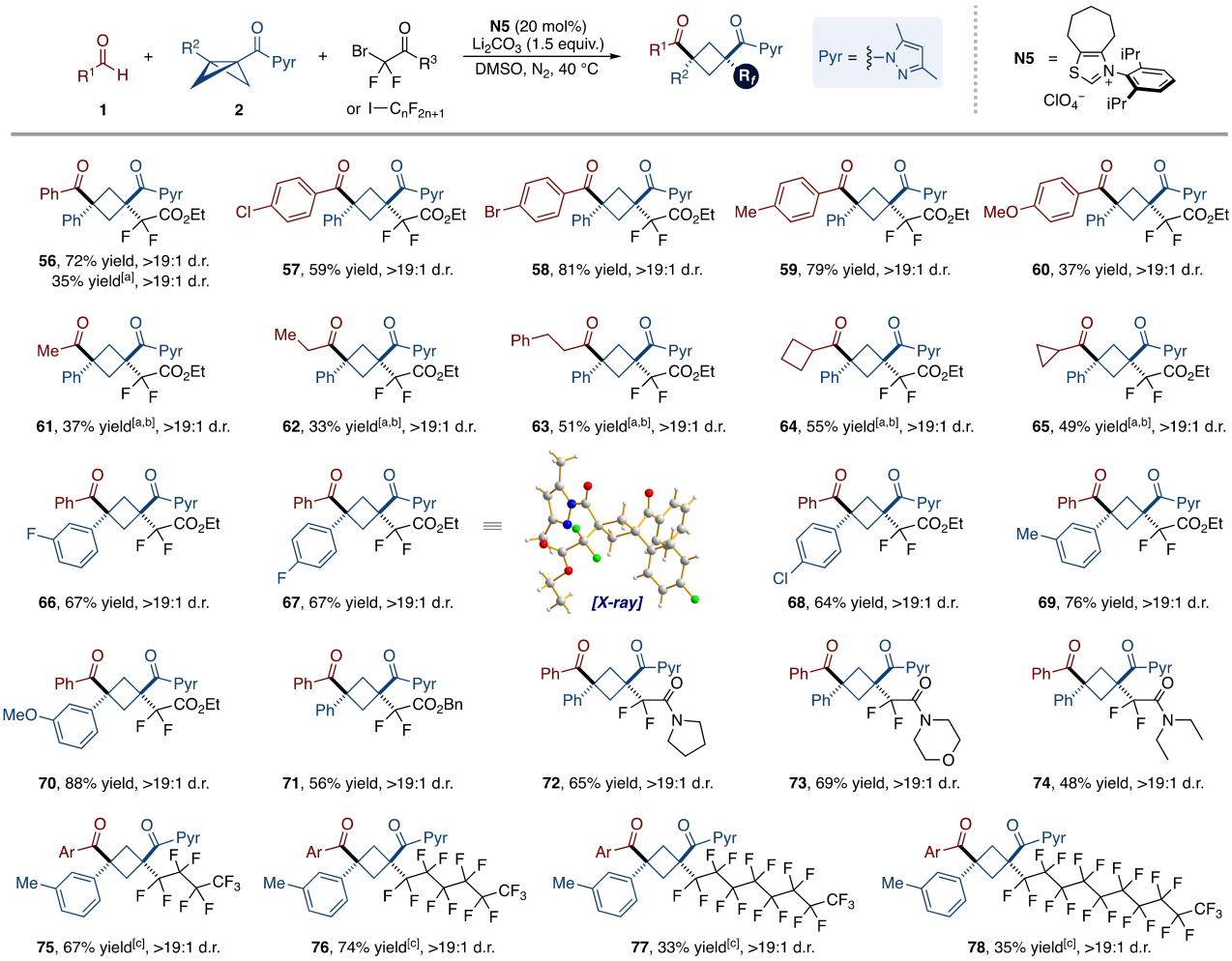

Scheme 3. Scope of Fluoroalkylating Reagents. Reactions generally performed with aldehyde **1** (0.15 mmol), bicyclobutane **2** (0.1 mmol), fluoroalkylating reagent **3** (0.2 mmol), NHC precatalyst **N5** (20 mol%) and Li_2CO_3 (1.5 equiv.) in DMSO (1.0 mL) at 40 °C for 18 h. Isolated product yields. D.r. values were determined by ^{1}H NMR. [a] Na_2CO_3 was used instead of Li_2CO_3. [b] NHC precatalyst **N1** was used instead of **N5**. [c] Cs_2CO_3 was used instead of Li_2CO_3, Ar = 4-Cl-C_6H_4.

between **IN3** and **IN6** proceeds via the open-shell singlet diradical **TS3** to form **IN7**, which undergoes facile NHC elimination to afford the major product **IN8** and regenerate NHC catalyst **N1'**. The NHC-bound ketyl radical **IN3** can potentially approach the benzyl radical **IN6** from two directions, namely, from the front of the cyclobutane (facing the *N*-acylpyrazole, **TS3**) or from the back (facing the trifluoromethyl group, **TS3'**). DFT calculations show that **TS3** has an energy barrier of 17.4 kcal/mol, while **TS3'** has a barrier of 20.9 kcal/mol, leading to the formation of the minor product **IN8'**. This difference in transition state energies ($\Delta\Delta G^{\ddagger}$ = 3.5 kcal/mol) is in accord with the experimental result that **4** (**IN8**) was isolated as major product.

Since the *front* approach in the radical-radical cross-coupling step is favored regardless of the substituents on the ketyl radical – despite the varying diastereomeric ratios (d.r.) for some substrates – we wished to understand the origin of this strong preference. Scheme 6 shows the favored transition state (**TS3**) in a blue frame. The preferred direction of approach by **IN3** in **TS3** is on the side of the dimethylpyrazolyl group and *anti* to the trifluoromethyl group. The analysis performed below suggests that this originates from 1) attractive dispersion and 2) repulsive electrostatic interactions between the two coupling species. The dimethylpyrazolyl group in **TS3** provides van der Waals or π–π interactions with the phenyl group on the ketyl radical, which likely enhances dispersive attraction and favors this transition state. In contrast, **TS3'** lacks this dispersion interaction.

We first explored the dispersion interactions by visual analysis of noncovalent interactions (NCIs)[19] using the independent gradient model based on Hirshfeld partition (IGMH).[20] As shown in Scheme 6, multiple C–H···π/van der Waals interactions are present between the two fragments (green blobs). The main regions of weak interactions within the two fragments are quite similar in both **TS3** and **TS3'**. However, a notable distinction is that in **TS3**, van der Waals

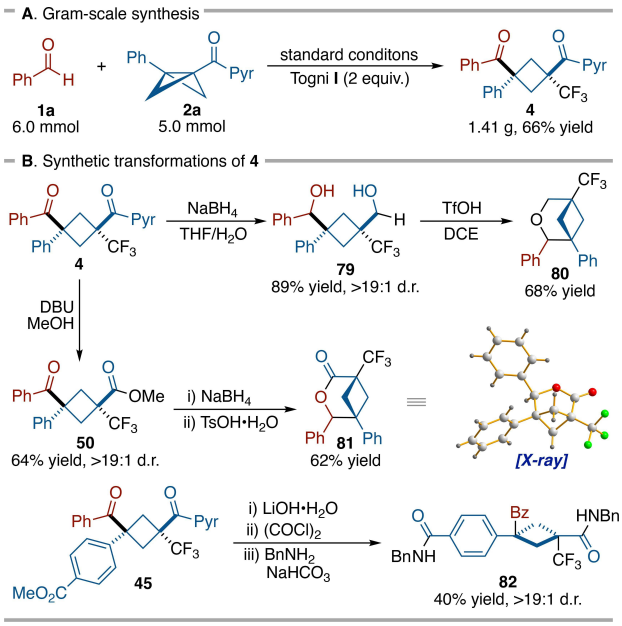

Scheme 4. Gram-scale synthesis and transformation of the product.

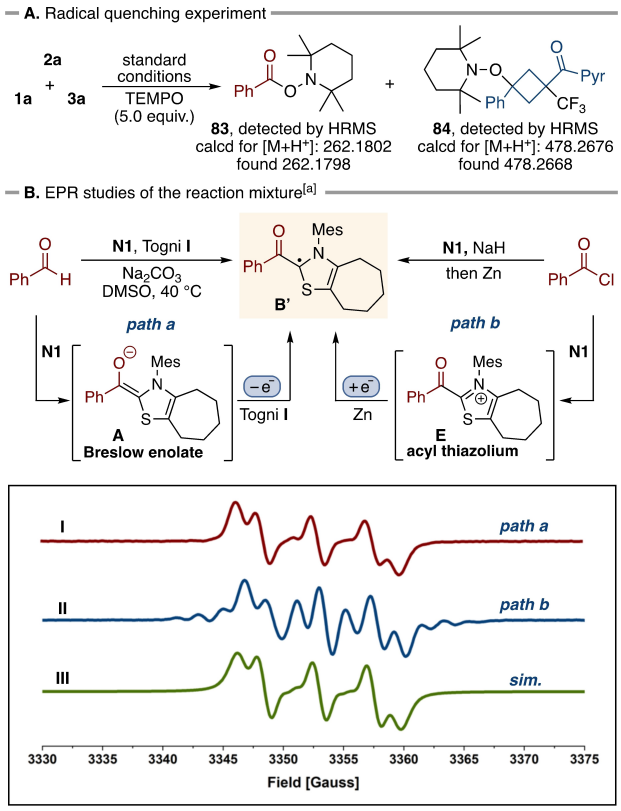

Scheme 5. Experimental mechanistic studies. [a] Experimental and simulated X-band EPR spectra of radical **B'** in the acylfluoroalkylation reaction. **I**. Reaction mixture of benzaldehyde **1a**, Togni **I** reagent, and **N1** (path a). **II**. Generation of radical **B'** via SET reduction of acylthiazolium intermediate (path b). **III**. Simulated EPR spectrum. $g = 2.0051$.

interactions occur between the dimethylpyrazolyl and phenyl groups.

Electrostatic interactions were also investigated. The two electronegative groups — specifically the trifluoromethyl group and the oxygen atom in the ketyl radical – are positioned in close proximity in the *back* approach (**TS3'**), and the electrostatic repulsion might hinder their approach towards each other. Electrostatic potential profiles were calculated and plotted on the van der Waals surface of the two fragments in both transition states.[21] As depicted in Scheme 6, for two separated fragments, the electronegative regions are clearly localized on the oxygen atom of the ketyl radical and the trifluoromethyl group (in red) while the electropositive regions are shown in blue. As the two fragments approach each other to form the transition state (right subfigures), the Coulombic interactions become evident. In particular, this is energetically favorable when the interacting colors are opposite, as observed in **TS3**. In contrast, the red electronegative regions are positioned "face-to-face" in **TS3'**, resulting in stronger electrostatic repulsion. Therefore, we believe that the preferred formation of **TS3** over **TS3'** is jointly determined by dispersion and electrostatic interactions.

To further investigate the dispersion and electrostatic effects induced by the substituents, we carried out calculations on three examples studied experimentally and three additional modified structures. Scheme 7 shows the two competing transition states for the formation of two stereoisomers in each case. Structures in Scheme 7A have been described in Scheme 6, where the strongest dispersion and electrostatic interactions exist. Replacing the dimethylpyrazolyl in **TS3** and **TS3'** with *N,O*-dimethylhydroxylamine decreases the energy difference from 3.5 kcal/mol to 2.5 kcal/mol (Scheme 7B). Replacing dimethylpyrazolyl with methyl ester leads to a further decrease in $\Delta\Delta G^{\ddagger}$, while still maintaining its diastereoselectivity (Scheme 7C). This is consistent with experiments for all three of the products (**4**, **49**, **50**). In order to minimize dispersion interactions, we replaced dimethylpyrazolyl with a hydrogen. As expected, the energy difference significantly decreases to 1.1 kcal/mol (Scheme 7D). Similarly, for electrostatic effects, we started by replacing the trifluoromethyl group with a methyl group, where the electrostatic repulsion with ketyl radical was notably weakened, reducing $\Delta\Delta G^{\ddagger}$ from 3.5 kcal/mol to 1.9 kcal/mol (Scheme 7E). Ultimately, to eliminate both dispersion and electrostatic interactions, we substituted dimethylpyrazolyl and trifluoromethyl groups with hydrogen and methyl, respectively; a complete loss of diastereoselectivity was observed (Scheme 7F). These results further demonstrate the critical roles of dispersion and electrostatic effects in determining diastereoselectivity.

Conclusion

We have developed a diastereoselective method for the acylfluoroalkylation of bicyclobutanes under NHC catalysis. The key to the success of this strategy is the formation of an NHC-bound ketyl radical with appropriate steric properties,

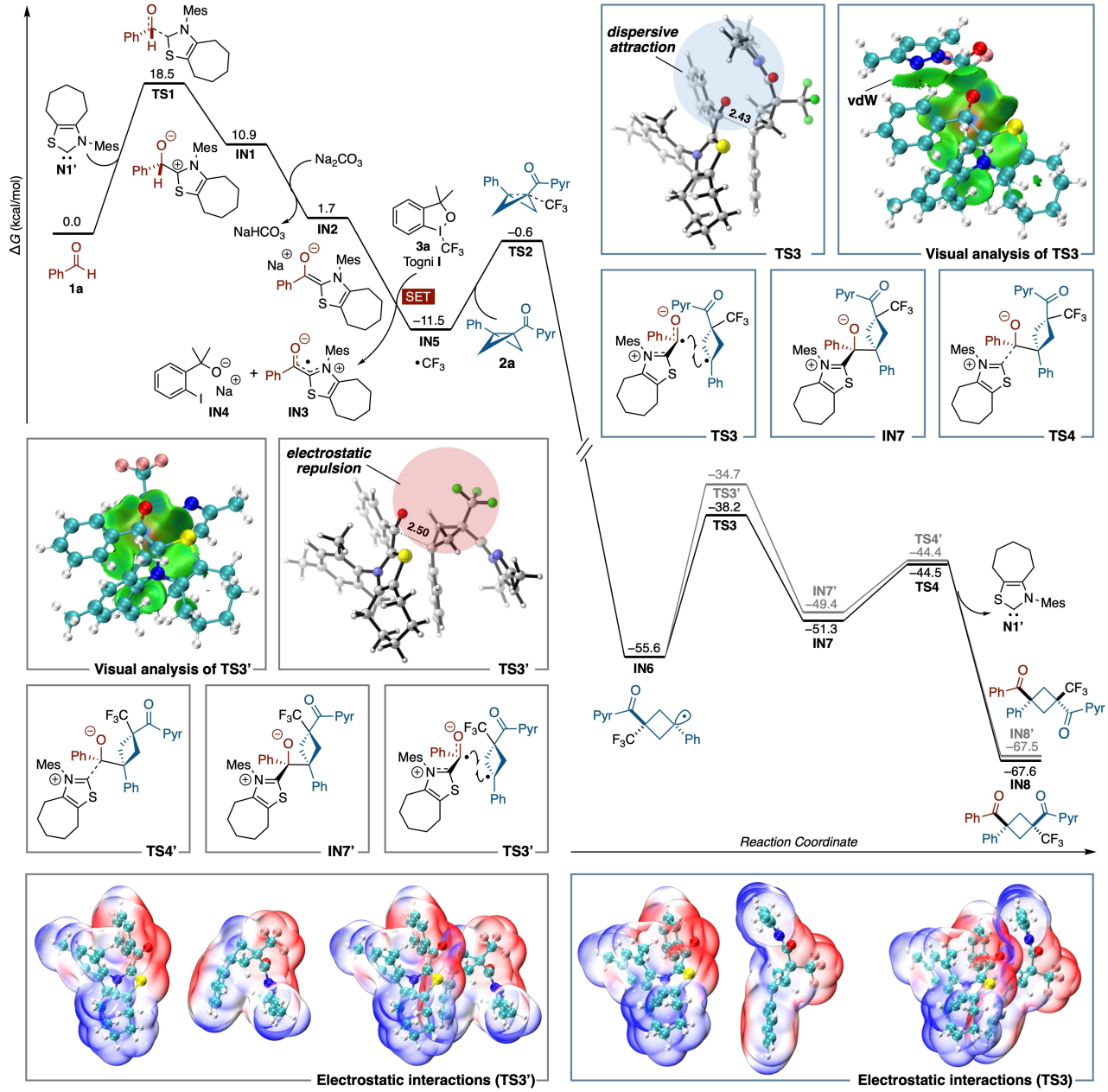

Scheme 6. Computational mechanistic studies. Computational studies were performed with (u)ωB97X–D/def2-tzvpp/SMD(DMSO)//(u)ωB97X–D/def2-svp/IEFPCM(DMSO) at 313.15 K with Grimme's entropic correction.[22] Structures of transition states were illustrated by CYLview.[23] Dispersive and electrostatic intereactions were analyzed in Multiwfn[24] and visualized in VMD.[25]

which has been confirmed by EPR spectroscopic studies. This method provides access to a series of 1,1,3,3-tetrasubstituted cyclobutanes that can be readily elaborated into bridged heterocycles. A detailed computational analysis of the catalytic system suggests that the exceptional stereoselectivity arises from dispersion and electrostatic interactions between the radical intermediates. Further application of this organocatalytic strategy to enantioselective radical-involved transformations are currently under investigation.

Acknowledgements

J.Z. is grateful for the financial support provided by the National Natural Science Foundation of China (No. 22371028). K.N.H. is grateful to the National Science Foundation (CHE-2153972 for K.N.H.) and computational resources from Expanse at SDSC through allocation CHE040014 from the Advanced Cyberinfrastructure Coordination Ecosystem: Services & Support (ACCESS) program (for K.N.H. and J.-R.S.). W. Wang is grateful to the National Key R&D Program of China (2022YFB4602505). We acknowledge the assistance of Dr. Huihui Wan in DUT

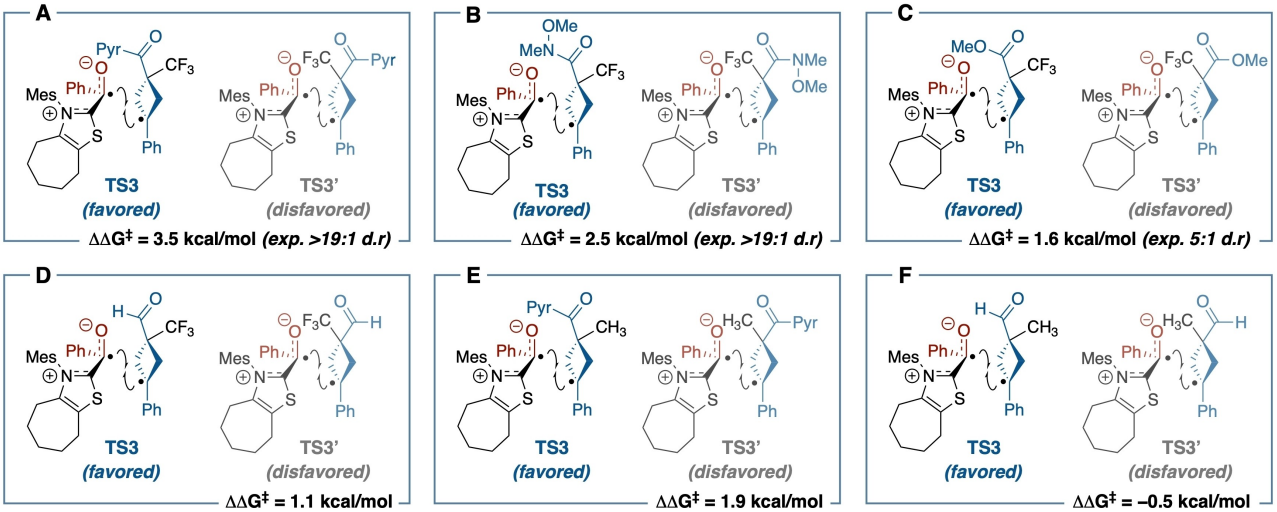

Scheme 7. Energy difference between **TS3** and **TS3'**. Computational studies are performed with (u)ωB97X–D/def2-tzvpp/SMD-(DMSO)//(u)ωB97X–D/def2-svp/IEFPCM(DMSO) at 313.15 K with Grimme's entropic correction.

Instrumental Analysis Center for her help with HRMS analysis.

Conflict of Interest

The authors declare no conflict of interest.

Data Availability Statement

The data that support the findings of this study are available in the supplementary material of this article.

Keywords: Cyclobutanes · Organocatalysis · Radicals · Stereoselectivity · Strain Release

[1] For selected reviews, see: a) V. M. Dembitsky, *Phytomedicine* **2014**, *21*, 1559–1581; b) Y.-Y. Fan, X.-H. Gao, J.-M. Yue, *Sci. China Chem.* **2016**, *59*, 1126–1141; c) M. A. Beniddir, L. Evanno, D. Joseph, A. Skiredj, E. Poupon, *Nat. Prod. Rep.* **2016**, *33*, 820–842.

[2] For selected reviews, see: a) M. R. Bauer, P. D. Fruscia, S. C. C. Lucas, I. N. Michaelides, J. E. Nelson, R. I. Storer, B. C. Whitehurst, *RSC Med. Chem.* **2021**, *12*, 448–471; b) M. R. van der Kolk, M. A. C. H. Janssen, F. P. J. T. Rutjes, D. Blanco-Ania, *ChemMedChem* **2022**, *17*, e202200020.

[3] For selected reviews regarding the synthesis of cyclobutanes, see: a) E. Lee-Ruff, G. Mladenova, *Chem. Rev.* **2003**, *103*, 1449–1483; b) J. Li, K. Gao, M. Bian, H. Ding, *Org. Chem. Front.* **2020**, *7*, 136–154; c) M. Mato, A. Franchino, C. García-Morales, A. M. Echavarren, *Chem. Rev.* **2021**, *121*, 8613–8684.

[4] For selected reviews on [2 + 2] cycloaddition reactions, see: a) T. Bach, *Synthesis* **1998**, 683–703; b) T. P. Yoon, *ACS Catal.* **2013**, *3*, 895–902; c) Y. Xu, M. L. Conner, M. K. Brown, *Angew. Chem. Int. Ed.* **2015**, *54*, 11918–11928; d) T. P. Yoon, *Acc. Chem. Res.* **2016**, *49*, 2307–2315; e) S. Poplata, A. Tröster, Y.-Q. Zou, T. Bach, *Chem. Rev.* **2016**, *116*, 9748–9815; f) R. Guo, M. K. Brown, *Acc. Chem. Res.* **2023**, *56*, 2253–2264.

[5] For selected reviews, see: a) M. A. A. Walczak, T. Krainz, P. Wipf, *Acc. Chem. Res.* **2015**, *48*, 1149–1158; b) A. Fawcett, *Pure Appl. Chem.* **2020**, *92*, 751–765; c) J. Turkowska, J. Durka, D. Gryko, *Chem. Commun.* **2020**, *56*, 5718–5734; d) C. B. Kelly, J. A. Milligan, L. J. Tilley, T. M. Sodano, *Chem. Sci.* **2022**, *13*, 11721–11737; e) M. Golfmann, J. C. L. Walker, *Commun. Chem.* **2023**, *6*, 9; f) J. L. Tyler, V. K. Aggarwal, *Chem. Eur. J.* **2023**, *29*, e202300008; g) P. Bellotti, F. Glorius, *J. Am. Chem. Soc.* **2023**, *145*, 20716–20732.

[6] For selected examples on the ring-opening of BCBs to form cyclobutanes, see: a) R. Panish, S. R. Chintala, D. T. Boruta, Y. Fang, M. T. Taylor, J. M. Fox, *J. Am. Chem. Soc.* **2013**, *135*, 9283–9286; b) R. Gianatassio, J. M. Lopchuk, J. Wang, C.-M. Pan, L. R. Malins, L. Prieto, T. A. Brandt, M. R. Collins, G. M. Gallego, N. W. Sach, J. E. Spangler, H. Zhu, J. Zhu, P. S. Baran, *Science* **2016**, *351*, 241–246; c) L. Guo, A. Noble, V. K. Aggarwal, *Angew. Chem. Int. Ed.* **2021**, *60*, 212–216; d) A. Guin, S. Bhattacharjee, M. S. Hararia, A. T. Biju, *Chem. Sci.* **2023**, *14*, 6585–6591; e) L. Tang, Q.-N. Huang, F. Wu, Y. Xiao, J.-L. Zhou, T.-T. Xu, W.-B. Wu, S. Qu, J.-J. Feng, *Chem. Sci.* **2023**, *14*, 9696–9703; f) A. Dasgupta, S. Bhattacharjee, Z. Tong, A. Guin, R. E. McNamee, K. E. Christensen, A. T. Biju, E. A. Anderson, *J. Am. Chem. Soc.* **2024**, *146*, 1196–1203; g) A. Fawcett, T. Biberger, V. K. Aggarwal, *Nat. Chem.* **2019**, *11*, 117–122; h) S. H. Bennett, A. Fawcett, E. H. Denton, T. Biberger, V. Fasano, N. Winter, V. K. Aggarwal, *J. Am. Chem. Soc.* **2020**, *142*, 16766–16775; i) H.-C. Shen, M. V. Popescu, Z.-S. Wang, L. de Lescure, A. Noble, R. S. Paton, V. K. Aggarwal, *J. Am. Chem. Soc.* **2023**, *145*, 16508–16516; j) B. Wölfl, N. Winter, J. Li, A. Noble, V. K. Aggarwal, *Angew. Chem. Int. Ed.* **2023**, *62*, e202217064; k) S.-L. Lin, Y.-H. Chen, H.-H. Liu, S.-H. Xiang, B. Tan, *J. Am. Chem. Soc.* **2023**, *145*, 21152–21158.

[7] a) G. Ernouf, E. Chirkin, L. Rhyman, P. Ramasami, J.-C. Cintrat, *Angew. Chem. Int. Ed.* **2020**, *59*, 2618–2622; b) M. Ociepa, A. J. Wierzba, J. Turkowska, D. Gryko, *J. Am. Chem. Soc.* **2020**, *142*, 5355–5361; c) M. Silvi, V. K. Aggarwal, *J. Am. Chem. Soc.* **2019**, *141*, 9511–9515; d) L. Lewis-Borrell, M. Sneha, I. P. Clark, V. Fasano, A. Noble, V. K. Aggarwal, A. J. Orr-Ewing, *J. Am. Chem. Soc.* **2021**, *143*, 17191–17199; e) H. Wang, J. E. Erchinger, M. Lenz, S. Dutta, C. G. Daniliuc, F. Glorius, *J. Am. Chem. Soc.* **2023**, *145*, 23771–23780; f) Y. Xiao,

T.-T. Xu, J.-L. Zhou, F. Wu, L. Tang, R.-Y. Liu, W.-B. Wu, J.-J. Feng, *Chem. Sci.* **2023**, *14*, 13060–13066.

[8] For selected recent examples on cyclization and insertion-type reactions of BCBs to form bridged bicyclic compounds, see: a) R. Kleinmans, T. Pinkert, S. Dutta, T. O. Paulisch, H. Keum, C. G. Daniliuc, F. Glorius, *Nature* **2022**, *605*, 477–482; b) H. Wang, H. Shao, A. Das, S. Dutta, H. T. Chan, C. Daniliuc, K. N. Houk, F. Glorius, *Science* **2023**, *381*, 75–81; c) S. Agasti, F. Beltran, E. Pye, N. Kaltsoyannis, G. E. M. Crisenza, D. J. Procter, *Nat. Chem.* **2023**, *15*, 535–541; d) R. Guo, Y.-C. Chang, L. Herter, C. Salome, S. E. Braley, T. C. Fessard, M. K. Brown, *J. Am. Chem. Soc.* **2022**, *144*, 7988–7994; e) Y. Zheng, W. Huang, R. K. Dhungana, A. Granados, S. Keess, M. Makvandi, G. A. Molander, *J. Am. Chem. Soc.* **2022**, *144*, 23685–23690; f) K. Dhake, K. J. Woelk, J. Becica, A. Un, S. E. Jenny, D. C. Leitch, *Angew. Chem. Int. Ed.* **2022**, *61*, e202204719; g) M. de Robichon, T. Kratz, F. Beyer, J. Zuber, C. Merten, T. Bach, *J. Am. Chem. Soc.* **2023**, *145*, 24466–24470; h) N. Radhoff, C. G. Daniliuc, A. Studer, *Angew. Chem. Int. Ed.* **2023**, *62*, e202304771; i) Y. Liang, F. Paulus, C. G. Daniliuc, F. Glorius, *Angew. Chem. Int. Ed.* **2023**, *62*, e202305043; j) D. Ni, S. Hu, X. Tan, Y. Yu, Z. Li, L. Deng, *Angew. Chem. Int. Ed.* **2023**, *62*, e202308606; k) S. Hu, Y. Pan, D. Ni, L. Deng, *Nat. Commun.* **2024**, *15*, 6128; l) Q. Fu, S. Cao, J. Wang, X. Lv, H. Wang, X. Zhao, Z. Jiang, *J. Am. Chem. Soc.* **2024**, *146*, 8372–8380.

[9] For selected reviews, see: a) T. Ishii, K. Nagao, H. Ohmiya, *Chem. Sci.* **2020**, *11*, 5630–5636; b) H. Ohmiya, *ACS Catal.* **2020**, *10*, 6862–6869; c) Q. Liu, X.-Y. Chen, *Org. Chem. Front.* **2020**, *7*, 2082–2087; d) J. Liu, X.-N. Xing, J.-H. Huang, L.-Q. Lu, W.-J. Xiao, *Chem. Sci.* **2020**, *11*, 10605–10613; e) L. Dai, S. Ye, *Chin. Chem. Lett.* **2021**, *32*, 660–667; f) Q.-Z. Li, R. Zeng, B. Han, J.-L. Li, *Chem. Eur. J.* **2021**, *27*, 3238–3250; g) A. V. Bay, K. A. Scheidt, *Trends Chem.* **2022**, *4*, 277–290; h) K. Liu, M. Schwenzer, A. Studer, *ACS Catal.* **2022**, *12*, 11984–11999; i) Q. Tang, D. Du, J. Gao, *Eur. J. Org. Chem.* **2023**, *26*, e202300832; j) X. Wang, S. Wu, R. Yang, H. Song, Y. Liu, Q. Wang, *Chem. Sci.* **2023**, *14*, 13367–13383; k) F. Lu, F. Su, S. Pan, X. Wu, X. Wu, Y. R. Chi, *Chem. Eur. J.* **2024**, *30*, e202401811.

[10] a) I. Nakanishi, S. Itoh, T. Suenobu, S. Fukuzumi, *Angew. Chem. Int. Ed.* **1998**, *37*, 992–994; b) L. Delfau, S. Nichilo, F. Molton, J. Broggi, E. Tomás-Mendivil, D. Martin, *Angew. Chem. Int. Ed.* **2021**, *60*, 26783–26789.

[11] For selected examples on radical NHC catalysis via oxidative process, see: a) T. Ishii, Y. Kakeno, K. Nagao, H. Ohmiya, *J. Am. Chem. Soc.* **2019**, *141*, 3854–3858; b) T. Ishii, K. Ota, K. Nagao, H. Ohmiya, *J. Am. Chem. Soc.* **2019**, *141*, 14073–14077; c) I. Kim, H. Im, H. Lee, S. Hong, *Chem. Sci.* **2020**, *11*, 3192–3197; d) J.-L. Li, Y.-Q. Liu, W.-L. Zou, R. Zeng, X. Zhang, Y. Liu, B. Han, Y. He, H.-J. Leng, Q.-Z. Li, *Angew. Chem. Int. Ed.* **2020**, *59*, 1863–1870; e) Q.-Z. Li, R. Zeng, Y. Fan, Y.-Q. Liu, T. Qi, X. Zhang, J.-L. Li, *Angew. Chem. Int. Ed.* **2022**, *61*, e202116629; f) Q.-Z. Li, Y.-Q. Liu, X.-X. Kou, W.-L. Zou, T. Qi, P. Xiang, J.-D. Xing, X. Zhang, J.-L. Li, *Angew. Chem. Int. Ed.* **2022**, *61*, e202207824; g) W.-D. Liu, W. Lee, H. Shu, C. Xiao, H. Xu, X. Chen, K. N. Houk, J. Zhao, *J. Am. Chem. Soc.* **2022**, *144*, 22767–22777; h) Q.-Z. Li, W.-L. Zou, Z.-Y. Yu, X.-X. Kou, Y.-Q. Liu, X. Zhang, Y. He, J.-L. Li, *Nat. Catal.* **2024**, *7*, 900–911.

[12] For selected examples on dual NHC/photocatalysis, see: a) A. Mavroskoufis, K. Rajes, P. Golz, A. Agrawal, V. Ruß, J. P. Götze, M. N. Hopkinson, *Angew. Chem. Int. Ed.* **2020**, *59*, 3190–3194; b) M.-S. Liu, W. Shu, *ACS Catal.* **2020**, *10*, 12960–12966; c) A. V. Bay, K. P. Fitzpatrick, G. A. González-Montiel, A. O. Farah, P. H.-Y. Cheong, K. A. Scheidt, *Angew. Chem. Int. Ed.* **2021**, *60*, 17925–17931; d) X. Yu, Q.-Y. Meng, C. G. Daniliuc, A. Studer, *J. Am. Chem. Soc.* **2022**, *144*, 7072–7079; e) S. Jin, X. Sui, G. C. Haug, V. D. Nguyen, H. T. Dang, H. D. Arman, O. V. Larionov, *ACS Catal.* **2022**, *12*, 285–294; f) C.-Y. Tan, M. Kim, S. Hong, *Angew. Chem. Int. Ed.* **2023**, *62*, e202306191; g) Y. Sato, Y. Miyamoto, T. Matsui, Y. Sumida, H. Ohmiya, *Chem Catal.* **2023**, *3*, 100736; h) Y. Goto, M. Sano, Y. Sumida, H. Ohmiya, *Nat. Synth.* **2023**, *2*, 1037–1045; i) S. Byun, M. U. Hwang, H. R. Wise, A. V. Bay, P. H.-Y. Cheong, K. A. Scheidt, *Angew. Chem. Int. Ed.* **2023**, *62*, e202312829; j) Y. Xu, H. Chen, L. Yu, X. Peng, J. Zhang, Z. Xing, Y. Bao, A. Liu, Y. Zhao, C. Tian, Y. Liang, X. Huang, *Nature* **2024**, *625*, 74–79.

[13] For NHC catalyzed fluoroalkylation reaction, see the following review and references therein: Z. Jin, F. Zhang, X. Xiao, N. Wang, X. Lv, L. Zhou, *Org. Chem. Front.* **2024**, *11*, 2112–2133.

[14] The NHC-bound ketyl radicals from *ortho*-substituted aromatic aldehyde are more congested and usually lead to unsuccessful radical – radical coupling.

[15] For a list of unsuccessful substrates, see the Supporting Information for details.

[16] For selected reviews, see: a) K. Müller, C. Faeh, F. Diederich, *Science* **2007**, *317*, 1881–1886; b) S. Purser, P. R. Moore, S. Swallow, V. Gouverneur, *Chem. Soc. Rev.* **2008**, *37*, 320–330; c) J. Wang, M. Sánchez-Roselló, J. L. Aceña, C. del Pozo, A. E. Sorochinsky, S. Fustero, V. A. Soloshonok, H. Liu, *Chem. Rev.* **2014**, *114*, 2432–2506.

[17] a) G. Morini, M. Comini, M. Rivara, S. Rivara, S. Lorenzi, F. Bordi, M. Mor, L. Flammini, S. Bertoni, V. Ballabeni, E. Barocelli, P. V. Plazzi, *Bioorg. Med. Chem. Lett.* **2006**, *16*, 4063–4067; b) T. T. Wager, B. A. Pettersen, A. W. Schmidt, D. K. Spracklin, S. Mente, T. W. Butler, H. Howard, D. J. Lettiere, D. M. Rubitski, D. F. Wong, F. M. Nedza, F. R. Nelson, H. Rollema, J. W. Raggon, J. Aubrecht, J. K. Freeman, J. M. Marcek, J. Cianfrogna, K. W. Cook, L. C. James, L. A. Chatman, P. A. Iredale, M. J. Banker, M. L. Homiski, J. B. Munzner, R. Y. Chandrasekaran, *J. Med. Chem.* **2011**, *54*, 7602–7620.

[18] a) J. Rehbein, S.-M. Ruser, J. Phan, *Chem. Sci.* **2015**, *6*, 6013–6018; b) V. Regnier, E. A. Romero, F. Molton, R. Jazzar, G. Bertrand, D. Martin, *J. Am. Chem. Soc.* **2019**, *141*, 1109–1117.

[19] a) S. Grimme, *Angew. Chem. Int. Ed.* **2008**, *47*, 3430–3434; b) A. J. Neel, M. J. Hilton, M. S. Sigman, F. D. Toste, *Nature* **2017**, *543*, 637–646.

[20] T. Lu, Q. Chen, *J. Comput. Chem.* **2022**, *43*, 539–555.

[21] T. Lu, F. Chen, *J. Mol. Graph. Model.* **2012**, *38*, 314–323.

[22] S. Grimme, *Chem. Eur. J.* **2012**, *18*, 9955–9964.

[23] CYLview20; C. Y. Legault, Université de Sherbrooke, 2020 (http://www.cylview.org).

[24] T. Lu, F. Chen, *J. Comput. Chem.* **2012**, *33*, 580–592.

[25] W. Humphrey, A. Dalke, K. Schulten, *J. Mol. Graphics* **1996**, *14*, 33–38.

[26] Deposition numbers 2301935 (for **4**), 2344505 (for **67**), and 2393704 (for **81**) contain the supplementary crystallographic data for this paper. These data are provided free of charge by the joint Cambridge Crystallographic Data Centre and Fachinformationszentrum Karlsruhe (CCDC).

Manuscript received: September 1, 2024
Accepted manuscript online: November 14, 2024
Version of record online: November 27, 2024